See Separate Sheet

LA-UR- 99–848

CONF-990602--

Title: ONLINE HIGH VOLTAGE POWER SUPPLY RIPPLE ESTIMATION
AND FEEDFORWARD IN LEDA

RECEIVED
MAY 0 3 1999
OSTI

Author(s): S. Kwon, A. Regan, Y-Ming Wang, T. Rohlev

Submitted to: American Control Conf., San Diego, CA
6/2-4/99

DISTRIBUTION OF THIS DOCUMENT IS UNLIMITED

MASTER

Los Alamos
NATIONAL LABORATORY

DISCLAIMER

DISCLAIMER

Portions of this document may be illegible in electronic image products. Images are produced from the best available original document.

Title: Online high voltage power supply ripple estimation and feedforward in LEDA

Authors: Sung-il Kwon, Amy Regan, Yi-Ming Wang, and Tony Rohlev
LLRF Technology Group
LANSCE-5
Los Alamos National Laboratory
E-mail : skwon@lanl.gov

Online high voltage power supply ripple estimation and feedforward in LEDA

Sung-il Kwon, Amy Regan, Y. M. Wang, and T. Rohlev
RF Technology Group
Accelerator Operations and Technology Division
Los Alamos National Laboratory
P.O.Box 1663
Los Alamos, NM 87544, USA
E-mail: skwon@lanl.gov

Abstract-The Low Energy Demonstration Accelerator(LEDA) being constructed at Los Alamos National Laboratory will serve as the prototype for the low energy section of Acceleration Production of Tritium(APT) accelerator. This paper addresses the problem of LLRF control system for LEDA. We propose an estimator of the ripple and its time derivative and a control law which is based on PID control and adaptive feedforward of estimated ripple. The control law reduces the effect of the deterministic cathode ripple that is due to high voltage power supply and achieves tracking of desired set points.

I. INTRODUCTION

The low energy demonstration accelerator(LEDA) for the Accelerator Production of Tritium(APT) is being built at Los Alamos National Laboratory. The primary function of the low level RF(LL RF) control system of LEDA is to control RF fields in the accelerating cavity and maintain field stability within ±1% peak to peak amplitude error and 1° peak to peak phase error[5].

This paper addresses the problem of LLRF control system attenuating the effect of ripple on the klystron cathode voltage that results from the high voltage power supply ripple. We propose a PID control law coupled with an adaptive feedforward of ripple estimate. The purpose of control is to reduce the effect of the deterministic cathode ripple that is due to harmonics of high voltage power supply[4] and is to achieve tracking of desired set points. Low frequency ripple does not deteriorate current LLRF control system performance based on current PID control methodology. As frequency of the ripple increases, however, the effect of the ripple on the performance increases too. Simulation shows that 0.3% high voltage power supply ripple yields 1.05° peak to peak phase error at about $72kHz$[3] and 1.0% high voltage power supply ripple yields 1.07° peak to peak phase error at about $20kHz$[7]. In order to suppress the high frequency ripple effect, the proposed controller makes use of a feedforward control coupled with a ripple estimator. The high voltage power supply ripple is coupled to the LEDA through a klystron. The effects of the ripple are on both the amplitude and the phase of a klystron. In [6],[7], the influences of the ripple are modeled by algebraic equations. A klystron is modeled by a nonlinear state space system[6],[7]. We, first, address two coordinate transformations of a klystron model. Based on new coordinates, we extract the ripple equation which is represented by algebraic equations of states of new coordinates. The ripple estimator proposed in this work is based on the algebraic equation and it estimates the ripple signal itself and the time derivative of the ripple as well. The estimate of ripple is feedforwarded to the current LLRF control system whose frame is a PID control. This simple addition of an adaptive feedforward greatly improves the closed loop system performance.

II. KLYSTRON MODEL

We consider a klystron model as shown in as shown in Figure 1.

It has two inputs, LLRF_I and LLRF_Q and two output HPRF_I and HPRF_Q. As intermediate outputs, Klystron has the normalized amplitude **N_AMPLITUDE** and the normalized phase **N_PHASE**.
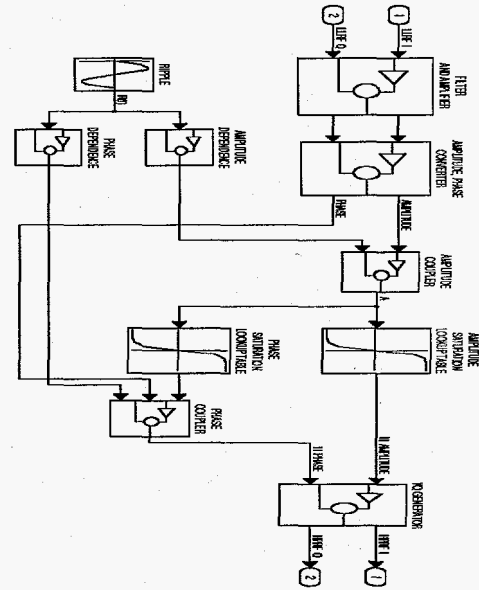
Figure 1. A Klystron Model

The first stage of a klystron are linear systems called **FILTER AND AMPLIFIER**. Let u_1=LLRF_I and let u_2=LLRF_Q. **FILTER AND AMPLIFIER** is represented in state space as

$$\dot{x}_1 = -a_1 x_1 + a_1 u_1 \qquad (1)$$

$$\dot{x}_2 = -a_1 x_2 + a_1 u_2 \qquad (2)$$

where $a_1 = \frac{1e^{+007}}{3.54}$.

A klystron model has two loop-up tables, called **AMPLITUDE SATURATION** and **PHASE SATURATION**. The input of the two look-up tables is given by

$$A = \frac{K_g}{10\sqrt{KP_m}}(0.01R(t)+1)^{1.25} \cdot \sqrt{x_1^2 + x_2^2} \qquad (3)$$

where $R(t)$ is the ripple, K_g is the klystron gain, and KP_m is the maximum klystron power. $R(t)$, K_g, and KP_m are specified for a given klystron. For given A, the output of the look-up table **AMPLITUDE SATURATION** can be represented by

$$A_N = I_1(A) \qquad (4)$$

and the output of the look-up table **PHASE SATURATION** can be represented by

$$\theta_N = I_2(A) \qquad (5)$$

Table 1 and table 2 show data of look-up table **AMPLITUDE SATURATION** and data of look-up table **PHASE SATURATION**, respectively.

The normalized amplitude **N_Amplitude**, defined by y_1^k and the normalized phase **N_Phase**, defined by y_2^k of the klystron are expressed by

$$y_1^k = A_N = I_1(A) \tag{6}$$

$$y_2^k = \theta_N + tan^{-1}(\frac{x_2}{x_1}) + 3 \cdot \frac{\pi}{180} \cdot R(t). \tag{7}$$

In addition, for given y_1^k and y_2^k, HPRF_I and HPRF_Q are given by

$$HPRF\_I = 10\sqrt{KP_m} \cdot y_1^k \cdot cos(y_2^k) \tag{8}$$

$$HPRF\_Q = 10\sqrt{KP_m} \cdot y_1^k \cdot sin(y_2^k). \tag{9}$$

A	A_N	A	A_N	A	A_N
-0.1000	0.0000	0.0700	0.0000	0.1400	0.1900
0.7100	0.8700	0.8600	0.9800	0.9000	1.0000
0.3122	0.4143	0.3568	0.4724	0.4014	0.5305
0.4907	0.6467	0.5353	0.7048	0.5799	0.7585
0.9100	1.0000	0.6468	0.8158	0.6691	0.8349
0.0446	0.0000	0.0892	0.0521	0.6914	0.8540
0.1338	0.1732	0.7806	0.9218	0.8252	0.9545
0.2230	0.2981	0.2676	0.3562	0.8921	0.9961
0.3122	0.4143	0.3568	0.4724	0.9813	0.9921

Table 1. AMPLITUDE SATURATION Data

A	θ_N	A	θ_N	A	θ_N
-0.1000	0.0000	0.0700	0.0000	0.6400	-0.0150
0.7100	-0.0350	0.0446	0.0000	0.6691	-0.0233
0.8600	-0.1370	0.9000	-0.2440	1.0000	-0.4770
0.4987	-0.0113	0.5445	-0.0125	0.5576	-0.0128
0.0892	-0.0005	0.1338	-0.0017	0.5712	-0.0132
0.1784	-0.0029	0.2230	-0.0040	0.8921	-0.2229
0.2676	-0.0052	0.3122	-0.0064	0.4483	-0.0100
0.3568	-0.0075	0.7885	-0.0884	0.9593	-0.3821

Table 2. PHASE SATURATION Data

Since the look-up tables have the limited number of data, we need to approximate the look-up tables by linear or nonlinear curve fitting equations. Considering the characteristic curve of a klystron, we choose nonlinear equations. We choose curve fitting equations of **AMPLITUDE SATURATION** and **PHASE SATURATION** having the forms

$$A_N = \sum_{i=1}^{N} c_i e^{-f_i A} \tag{10}$$

$$\theta_N = \sum_{i=1}^{N} d_i e^{-f_i A} \tag{11}$$

where f_i, $i = 1, 2, \cdots, N$ and parameters c_i, $i = 1, 2, \cdots, N$, d_i, $i = 1, 2, \cdots, N$ are to be determined.

Higher order of a curve fitting equation may yield more accurate curve fitting equation. For simplicity, we choose $N = 7$. Also, in order to reduce the number of coefficients to be determined, f_i, $i = 1, 2, \cdots, N$ are given in Table 3.

f_1	f_2	f_3	f_4	f_5	f_6	f_7
0.50	0.75	1.00	1.25	1.50	1.75	2.00

Table 3. Exponents of curve fitting equations

c_1	0.0568043e+006	d_1	-0.1412074e+005
c_2	-0.3926436e+006	d_2	0.8308426e+005
c_3	1.1280559e+006	d_3	-2.0177823e+005
c_4	-1.7241855e+006	d_4	2.5844141e+005
c_5	1.4787824e+006	d_5	-1.8368060e+005
c_6	-0.6748367e+006	d_6	0.6845313e+005
c_7	0.1280230e+006	d_7	-0.1039925e+005

Table 4. Coefficients of curve fitting equations

By using data given in Table 1 and Table 2, we obtain coefficients c_i, $i = 1, 2, \cdots, N$ and d_i, $i = 1, 2, \cdots, N$, of the curve fitting equations (10) and (11). Coefficients c_i and d_i obtained are given in Table 4.

Plugging (3) to (10) and (11), curve fitting equations (10) and (11) are reduced to

$$A_N = \sum_{i=1}^{N} c_i e^{-f_i w(t)\sqrt{x_1^2+x_2^2}} \tag{12}$$

$$\theta_N = \sum_{i=1}^{N} d_i e^{-f_i w(t)\sqrt{x_1^2+x_2^2}} \tag{13}$$

where

$$w(t) = \frac{K_g}{10\sqrt{KP_m}}(0.01R(t) + 1)^{1.25}. \tag{14}$$

The normalized amplitude y_1^k and the normalized phase y_2^k of the klystron are

$$y_1^k = \sum_{i=1}^{N} c_i e^{-f_i w(t)\sqrt{x_1^2+x_2^2}} \tag{15}$$

$$y_2^k = \sum_{i=1}^{N} d_i e^{-f_i w(t)\sqrt{x_1^2+x_2^2}} + tan^{-1}(\frac{x_2}{x_1}) + 3 \cdot \frac{\pi}{180} \cdot R(t). \tag{16}$$

II-A. THE KLYSTRON IN z-COORDINATE

Consider the normalized amplitude y_1^k and the normalized phase y_2^k as given in (15) and (16).

Let

$$z_1 = \sqrt{x_1^2+x_2^2} \tag{17}$$

$$z_2 = tan^{-1}(\frac{x_2}{x_1}). \tag{18}$$

We consider a transformation from x-coordinate to z-coordinate. In z-coordinate, the state equations (1) and (2) are reduced to

$$\dot{z_1} = -a_1 z_1 + a_1 cos(z_2)u_1 + a_1 sin(z_2)u_2 \tag{19}$$

$$\dot{z_2} = -a_1 \frac{sin(z_2)}{z_1}u_1 + a_1 \frac{cos(z_2)}{z_1}u_2. \tag{20}$$

Also, the curve fitting equations (10) and (11) are reduced to

$$A_N = \sum_{i=1}^{N} c_i e^{-f_i w(t)z_1} \tag{21}$$

$$\theta_N = \sum_{i=1}^{N} d_i e^{-f_i w(t)z_1}. \tag{22}$$

The normalized amplitude y_1^k and the normalized phase y_2^k are represented by

$$y_1^k = \sum_{i=1}^{N} c_i e^{-f_i w(t)z_1} \tag{23}$$

$$y_2^k = \sum_{i=1}^{N} d_i e^{-f_i w(t)z_1} + z_2 + 3 \cdot \frac{\pi}{180} \cdot R(t). \tag{24}$$

Note that the exponents of the first term of (23) are the same as the exponents of the first term of (24). Also, note that the phase y_2^k is linear with respect to z_2.

II-B. THE KLYSTRON IN $\overline{z}$-COORDINATE

Consider the Klystron equation in z-coordinate given in previous section.
Define

$$\overline{z}_1 = (0.01R(t) + 1)^{1.25} z_1 \tag{25}$$

$$\overline{z}_2 = z_2 + 3 \cdot \frac{\pi}{180} \cdot R(t). \tag{26}$$

The Klystron is expressed in $\overline{z}$-coordinate by

$$\dot{\overline{z}}_1 = -\overline{a}_1 \overline{z}_1 + b_{z11}(\overline{z}, R(t), \dot{R}(t)) u_1 + b_{z12}(\overline{z}, R(t), \dot{R}(t)) u_2$$
$$+ E_{z1}(R(t), \dot{R}(t)) \tag{27}$$

$$\dot{\overline{z}}_2 = b_{z21}(\overline{z}, R(t), \dot{R}(t)) u_1 + b_{z22}(\overline{z}, R(t), \dot{R}(t)) u_2$$
$$+ E_{z2}(R(t), \dot{R}(t)) \tag{28}$$

$$y_1^k = \sum_{i=1}^{N} c_i e^{-f_i M \overline{z}_1} \tag{29}$$

$$y_2^k = \sum_{i=1}^{N} d_i e^{-f_i M \overline{z}_1} + \overline{z}_2. \tag{30}$$

where
$\overline{a}_1 = a_1 - 0.0125(0.01R(t) + 1)^{-1} \dot{R}(t)$
$b_{z11}(\overline{z}, R(t), \dot{R}(t)) = a_1(0.01R(t) + 1)^{1.25} cos(\overline{z}_2 - 3 \cdot \frac{\pi}{180} \cdot R(t))$
$b_{z12}(\overline{z}, R(t), \dot{R}(t)) = a_1(0.01R(t) + 1)^{1.25} sin(\overline{z}_2 - 3 \cdot \frac{\pi}{180} \cdot R(t))$
$b_{z21}(\overline{z}, R(t), \dot{R}(t)) = -a_1 \frac{sin(\overline{z}_2 - 3 \cdot \frac{\pi}{180} \cdot R(t))}{\overline{z}_1}$
$b_{z22}(\overline{z}, R(t), \dot{R}(t)) = a_1 \frac{cos(\overline{z}_2 - 3 \cdot \frac{\pi}{180} \cdot R(t))}{\overline{z}_1}$
$E_{z1}(R(t), \dot{R}(t)) = 0$
$E_{z2}(R(t), \dot{R}(t)) = 3 \cdot \frac{\pi}{180} \dot{R}(t)$
$M = \frac{K_g}{10\sqrt{KP_m}}.$

Note that $\overline{B}_z(\overline{z}, R(t), \dot{R}(t))$ is invertible for any nonzero $\overline{z}_1$. In $\overline{z}$-coordinate, state equations are dependent upon the ripple $R(t)$ but the output equations are independent upon the ripple $R(t)$.

III. THE RF CAVITY

Figure 2 shows the RF cavity model.
RF cavity has four inputs, HPRF_I, HPRF_Q, BEAM_I, and BEAM_Q, two outputs, CAV_FLD_I and CAV_FLD_Q.
Let u_1^c=HPRF_I, u_2^c=HPRF_Q, u_3^c=BEAM_I, u_4^c=BEAM_Q and let y_1^c=CAV_FLD_I,
y_2^c=CAV_FLD_Q. Then, the RF cavity can be expressed in the state space form.

$$\dot{x} = Ax + Bu^c \tag{31}$$

$$y^c = Cx. \tag{32}$$

System matrices A, B, C of RF cavity are given in [3].

Also, FLD_I and FLD_Q of the cavity Field Sample System are given by

$$FLD\_I = FA \cdot cos(GD) \cdot y_1^c - FA \cdot sin(GD) \cdot y_2^c \tag{33}$$

$$FLD\_Q = FA \cdot sin(GD) \cdot y_1^c + FA \cdot cos(GD) \cdot y_2^c \tag{34}$$

and FLD_AMP and FLD_PHS of the cavity Field Sample System are given by

$$FLD\_AMP = \sqrt{FLD\_I^2 + FLD\_Q^2}$$

$$FLD\_PHS = tan^{-1}(\frac{FLD\_Q}{FLD\_I})$$

where

$$FA = 0.00037809$$
$$GD = \frac{\pi}{180} \cdot (-0.039455).$$

The RF cavity as given in (31), (32) is Hurwitz stable and is inverse stable as well.
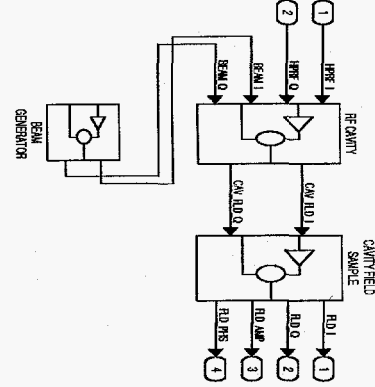

Figure 2. A RF cavity Model and a cavity Field Sample System

IV. RIPPLE ESTIMATION

The purpose of the low level RF control(LLRF) system is to maintain the field stability within $\pm 1.0\%$ amplitude and $1.0°$ phase. The present LLRF control system is based on PID control[4],[5]. As has been investigated in [3],[7], the high voltage power supply ripple has influence on the LLRF PID control system. Low frequency ripple does not deteriorate the performance of the closed loop system seriously but high frequency ripple deteriorates the performance of the closed loop system seriously.

For the remedy to the poor performance of the PID controlled LLRF control system due to the high frequency high voltage power supply ripple, we propose a feedforward control of the estimate of the ripple. The feedforward improves the performance significantly[1],[6].

In this section, we address the ripple estimator which estimates the ripple $R(t)$ and its time derivative $\frac{dR(t)}{dt}$.

We first consider equations as given in (17) and (18).

$$z_1 = \sqrt{x_1^2 + x_2^2} \tag{35}$$

$$z_2 = tan^{-1}(\frac{x_2}{x_1}) \tag{36}$$

where x_1 and x_2 satisfy

$$\dot{x}_1 = -a_1 x_1 + a_1 u_1 \tag{37}$$

$$\dot{x}_2 = -a_1 x_2 + a_1 u_2 \tag{38}$$

and u_1=LLRF_I, u_2=LLRF_Q. Given LLRF_I and LLRF_Q, we can obtain z_1 and z_2 by solving differential equations (37), (38) and algebraic equations (35), (36).

Second, we consider equations given by (8) and (9).

$$HPRF\_I = 10\sqrt{KP_m} \cdot y_1^k \cdot cos(y_2^k) \tag{39}$$

$$HPRF\_Q = 10\sqrt{KP_m} \cdot y_1^k \cdot sin(y_2^k). \tag{40}$$

From (39) and (40), for given HPRF_I and HPRF_Q, we obtain the normalized amplitude y_1^k and the normalized phase y_2^k of the klystron by solving algebraic equations.

$$y_1^k = \frac{1}{10\sqrt{KP_m}} \sqrt{HPRF\_I^2 + HPRF\_Q^2} \tag{41}$$

$$y_2^k = tan^{-1}(\frac{HPRF\_Q}{HPRF\_I}). \tag{42}$$

Third, we consider the klystron model as given in Figure 1. In Figure 1, the normalized amplitude of the klystron is the output of the look-up table **AMPLITUDE SATURATION**. The input of the look-up table **AMPLITUDE SATURATION** is given by

$$A = \frac{K_g}{10\sqrt{KP_m}}(0.01R(t) + 1)^{1.25} \cdot z_1 \qquad (43)$$

in z-coordinate, or

$$A = \frac{K_g}{10\sqrt{KP_m}}\overline{z}_1 \qquad (44)$$

in $\overline{z}$-coordinate. Also, there exists a region of (A, y_1^k) pairs where there is an inverse look-up table of the look-up table **AMPLITUDE SATURATION**. This region can be extracted from data given in Table 1 and Table 2. As in the case of **AMPLITUDE SATURATION**, we obtain the curve fitting equation for the inverse look-up table for **AMPLITUDE SATURATION**. Since, in controller design, we make use of the output equations (23) and (24) or (29) and (30) which are based on the curve fitting equation, in order to obtain the curve fitting equation for the inverse look-up table for **AMPLITUDE SATURATION** within the region of invertibility, we use the output equation as given in (29). Based on the generated data pairs from (29) where the selected data of y_1^k and $\overline{z}_1$ guarantee invertibility, we obtain the curve fitting equation as follows.

$$\overline{z}_1 = \sum_{i=1}^{N} c_i^z e^{-f_i^z y_1^k} \qquad (45)$$

where $N = 7$, coefficients f_i^z, $i = 1, 2, \cdots, N$ are given and the coefficients c_i^z, $i = 1, 2, \cdots, N$ are obtained by applying the optimization toolbox of Matlab/Simulink. Table 5 gives the data of the coefficients of the curve fitting. The nonlinear least square algorithm in Matlab/Simulink guarantees 1% accuracy of the curve fitting.

f_i^z		c_i^z	
f_1^z	0.50	c_1^z	246379.7012736
f_2^z	0.75	c_2^z	-1633291.8595640
f_3^z	1.00	c_3^z	4505197.5753121
f_4^z	1.25	c_4^z	-6618176.9543979
f_5^z	1.50	c_5^z	5460679.7305035
f_6^z	1.75	c_6^z	-2399431.1109898
f_7^z	2.00	c_7^z	438643.01506646

Table 5. Coefficients of Curve fitting equation for Inverse **AMPLITUDE SATURATION**

The estimate of the ripple $R(t)$ and the estimate of the time derivative $\frac{dR(t)}{dt}$ of the ripple $R(t)$ are obtained by considering the klystron system both in z-coordinate and $\overline{z}$-coordinate. The relation between z-coordinate and $\overline{z}$-coordinate is given by

$$\overline{z}_1 = (0.01R(t) + 1)^{1.25} z_1 \qquad (46)$$

$$\overline{z}_2 = z_2 + 3 \cdot \frac{\pi}{180} \cdot R(t). \qquad (47)$$

Whenever x_1 and x_2 are obtained from (37) and (38), then we can obtain z_1 by using (35), and also whenever y_1^k is obtained from (41), we can obtain $\overline{z}_1$ by using (45). For given z_1 and $\overline{z}_1$, we can obtain the estimate $\hat{R}(t)$ of the ripple $R(t)$ by solving algebraic equation (46).

$$\hat{R}(t) = 100((\frac{\overline{z}_1(t)}{z_1(t)})^{0.8} - 1.0). \qquad (48)$$

Also, the estimate $\dot{\hat{R}}(t)$ of time derivative $\dot{R}(t)$ of the ripple $R(t)$ is obtained by differentiation of $\hat{R}(t)$.

V. Feedforward Control of the estimate $\hat{R}(t)$

The work in [7] shows that the **AMPLITUDE DEPENDENCE** of the high voltage power supply ripple is not seriously effective to the performance of tracking set points of the LLRF control system. The main effect of the high voltage power supply ripple is due to **PHASE DEPENDENCE**.

In this section, we propose a feedforward control of the estimate $\hat{R}(t)$. The feedforward control improves the tracking performance of the field phase significantly.

We consider the output equations as given in (23), (24) and (39), (40). The amplitude and the phase of the high power RF(HPRF) amplifier are

$$HPRF\_AMP = \sqrt{HPRF\_I^2 + HPRF\_Q^2} \qquad (49)$$

$$HPRF\_PHS = tan^{-1}(\frac{HPRF\_Q}{HPRF\_I}). \qquad (50)$$

In (24), the normalized phase y_2^k is affected by the **PHASE DEPENDENCE** term

$$3 \cdot \frac{\pi}{180} \cdot R(t). \qquad (51)$$

When $R(t)$ is estimated within a satisfactory accuracy, a feedforward control loop from the estimate $\hat{R}(t)$ to $y_2^k(t)$ can attenuate the effect the high voltage power supply ripple $R(t)$ to the phase of the klystron and so the phase of field.

Define a feedforward loop gain from the estimate $\hat{R}(t)$ as

$$-3 \cdot \frac{\pi}{180} \qquad (52)$$

and consider $\overline{HPRF\_AMP}$, $\overline{HPRF\_PHS}$ defined by

$$\overline{HPRF\_AMP} = HPRF\_AMP \qquad (53)$$

$$\overline{HPRF\_PHS} = HPRF\_PHS - 3 \cdot \frac{\pi}{180} \cdot \hat{R}(t). \qquad (54)$$

Plugging (24), (42), and (50) into (54), we obtain

$$\overline{HPRF\_PHS} = y_2^k - 3 \cdot \frac{\pi}{180} \cdot \hat{R}(t)$$

$$= \sum_{i=1}^{N} d_i e^{-f_i w(t) z_1} + z_2 + 3 \cdot \frac{\pi}{180} \cdot R(t) - 3 \cdot \frac{\pi}{180} \cdot \hat{R}(t)$$

$$= \sum_{i=1}^{N} d_i e^{-f_i w(t) z_1} + z_2 + 3 \cdot \frac{\pi}{180}(R(t) - \hat{R}(t)). \qquad (55)$$

The estimate $\hat{R}(t)$ as given in (48) is defined by the solution of an algebraic equation (46). z_1 is given by (35) whose variables are the state of the exactly same system of **FILTER AND AMPLIFIER** of a klystron. $\overline{z}_1$ is given by the curve fitting equation (59) of the lookup table of inverse **AMPLITUDE SATURATION**.

Of course, we have to consider the **AMPLITUDE DEPENDENCE** represented by $(0.01R(t) + 1)^{1.25}$(1%ripple). However, this amount does not have an influence on the phase of the field significantly[3],[7].

From (53) and (54), we reconstruct M_HPRF_I and M_HPRF_Q which drive the RF cavity.

$$M\_HPRF\_I = \overline{HPRF\_AMP} \cdot cos(\overline{HPRF\_PHS}) \qquad (56)$$

$$M\_HPRF\_Q = \overline{HPRF\_AMP} \cdot sin(\overline{HPRF\_PHS}). \qquad (57)$$

Figure 3-4 show the simulation results of the proposed LLRF Control System with adaptive feedforward of the estimate $\hat{R}(t)$. The ripple is

$$R(t) = sin(2\pi ft), \qquad f = 40kHz.$$

The peak-to-peak amplitude error is 0.864% and the peak-to-peak phase error at steady state is 0.0474°. In order to compare the performance, we also simulate the closed loop system without the feedforward of the estimate $\hat{R}(t)$(Figure 5). The peak-to-peak amplitude error is 0.922% and the peak-to-peak phase error at steady state is 2.0752°. The peak-to-peak amplitude error is not much reduced with feedforward but the peak-to-peak phase error is greatly reduced(438% improvement).

References

[1] K. J. Astrom and T. Hagglund, *PID controllers:theory, design, and tuning*, Second Edition, Instrument Society of America, Research Triangle Park, NC, 1995.

[2] C.T. Chen, *Introduction to linear System Theory*, Second edition, Rinehart and Winston, New York, 1986.

[3] Sung-il Kwon, " 0.3% high voltage power supply ripple response test," *preprint*.

[4] D. Rees, J. Bradley III, K. Cummings, M. Lynch, A. Regan, T. Rohlev, W. Roybal, Y.M. Wang, "Design and test results of the low energy demonstration accelerator(LEDA) RF systems," *presented in XIX International LINAC Conference*, Chicago, USA, 1998.

[5] A. Regan and C. Ziomek, "APT LLRF control system model results," *presented in XIX International LINAC Conference*, Chicago, USA, 1998.

[6] Chris Ziomek and Amy Regan, "Simplification of Matrixx Model: Preliminary LLRF System Design," *Technical Note*, AOT-5-TN:001, RF Technology Group, AOT Division, Los Alamos National Laboratory, 1996.

[7] Chris Ziomek and Amy Regan, "Superconducting system model; HVPS ripple model," *Technical Note*, AOT-5-TN:003, RF Technology Group, AOT Division, Los Alamos National Laboratory, 1996.
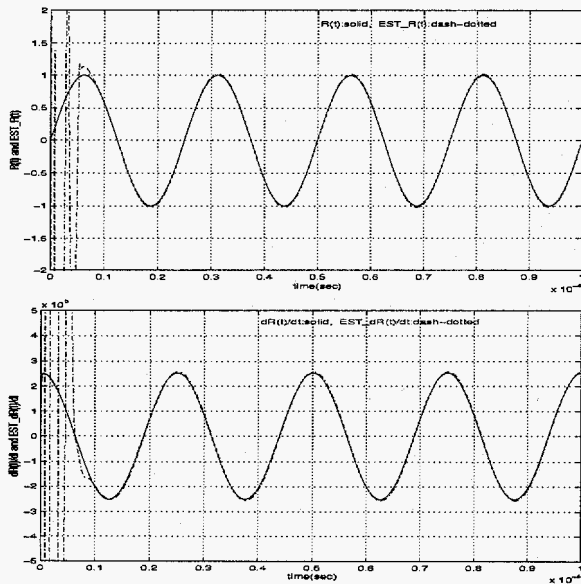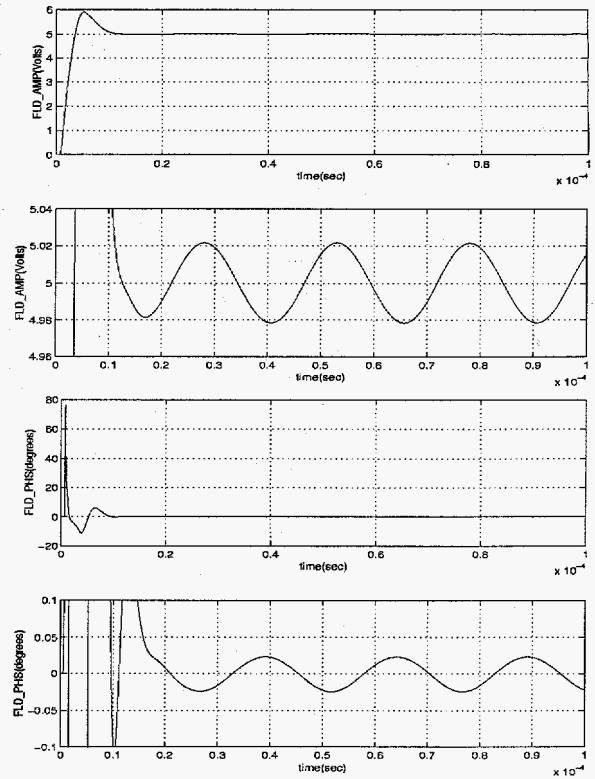
Figure 4. Amplitude of Field, FLD_AMP and Phase of Field, FLD_PHS with feedforward control of the Estimate $\hat{R}(t)$

Figure 3. Ripple $R(t)$ and its time derivative $dR(t)/dt$ and their estimates $EST\_R(t)$ and $EST\_dR(t)/dt$
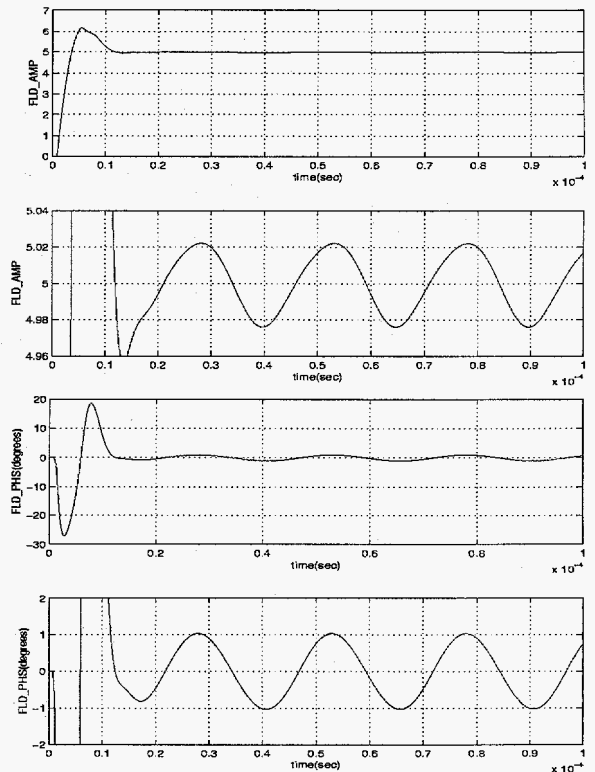

Figure 5. Amplitude of Field, FLD_AMP and Phase of Field, FLD_PHS without feedforward control